Effects of Irradiation Environment on V–4Cr–4Ti Alloys*)

Hideo WATANABE, Takeo MUROGA[1)] and Takuya NAGASAKA[1)]

Research Institute for Applied Mechanics, Kyushu University, 6-1 Kasuga-kouenn, Kasugashi, Fukuoka 816-8580, Japan
[1)]*National Institute for Fusion Science, 322-6 Oroshi, Toki, Gifu 509-5292, Japan*

(Received 7 December 2015 / Accepted 6 September 2016)

The effects of oxygen pick-up in an irradiation environment in a vacuum chamber during ion- and neutron-irradiation of V–4Cr–4Ti alloys were studied. The density and size of titanium oxides in the alloys were found to drastically increase because of the oxygen pick-up, especially for cases of higher irradiation dose and specimen temperature. Using Zr foil as a diffusion barrier and doping the V–4Cr–4Ti alloys with Y can be considered as effective techniques for reducing the reaction of Ti with C, O, and N to form Ti(C,O,N) because of oxygen-pick up from irradiation environment.

Keywords: vanadium–chromium–titanium alloy, irradiation, oxygen, environmental effects, titanium oxide

DOI: 10.1585/pfr.12.2405011

1. Introduction

V–4Cr–4Ti alloy is widely recognized for use as a fusion blanket structural material that is exposed to vacuum and helium gas, containing oxygen with low partial pressure. Interstitial impurities such as oxygen, carbon, and nitrogen are known to be important for radiation effects such as microstructure changes, irradiation hardening, and embrittlement [1–3]. In particular, oxygen is known to effectively influence the alloy properties. Ion-irradiation experiments conducted by the authors on V–4Cr–4Ti alloys at 473 - 973 K indicated that oxygen pick-up from the irradiation environment (namely, vacuum) is negligible, i.e., of the order of approximately 1 dpa [4, 5]. However, for higher irradiation dose levels, the effects might cause degradation of mechanical properties because of enhanced formation of titanium-oxide precipitates during irradiation [6, 7]. To understand the radiation-induced phenomena related to oxygen, such as oxide formation in the matrix, the oxygen level in the vanadium alloy as well as the oxygen pick-up from the radiation environment must be considered. Environmental effects on irradiation creep [8, 9], irradiation-induced hardness [10], and precipitation during neutron irradiation [11] have also been studied. Fukumoto *et al.* [8, 9] reported that the effect of sodium (Na) and lithium (Li) environment on creep behavior owing to the mass transfer of interstitial impurities was negligible. Hatakeyama *et al.* [12, 13] recently reported that the chemical composition of Ti(C,O,N) precipitates in a He environment was estimated as $V_{39}CrTiCO_3$ at 333 K and 673 K irradiation conditions in the Belgian Reactor 2 (BR2) and Japan Materials Testing Reactor (JMTR). The vanadium-enriched Ti(C,O,N) precipitates induced by the irradiation were affected by the mobility of point defects, i.e., interstitial inclusions and vacancies), and also by dislocation-loop formation at lower temperature ranges. Therefore, the objective of the present study is to understand the detailed mechanisms of oxygen pick-up from the irradiation environment in relation to the formation of titanium oxides.

2. Experimental Procedure

In this study, the results of irradiation for a sample of V–4Cr–4Ti alloy with a welded joint are summarized. The irradiation was performed for heavy ions using a tandem accelerator and fission neutrons in JMTR. For the ion irradiation, joint samples welded using a Yttrium–aluminium–garnet laser were used in this study. These samples were prepared from a high-purity V–4Cr–4Ti alloy, designated as NIFS-HEAT2 [14, 15]. Before welding (bead-on-plate welding) in a high-purity argon atmosphere, the samples were annealed in a vacuum at 1,273 K for 2 h. The detailed procedure for the welding has been reported in a previous study [16]. Oxygen concentrations of the samples before welding and that of the welded metal were 139 and 158 wt ppm, respectively. The samples were subjected to 2.4 MeV copper-ion irradiation using a tandem accelerator at Kyushu University. Transmission electron microscopy (TEM) specimens were sliced from welded materials and irradiated at 573 K and 873 K up to doses of 12 dpa. After irradiation, the specimens were electropolished using a back-thinning method, and the area near the peak-damage region (at approximately 700 nm) was observed by TEM. The TEM samples were also prepared by focused ion beams (FIB) using 30 keV Ga ions to obtain cross-sectional views of the samples.

For neutron irradiation in JMTR, arc-melted V–4Cr–4Ti alloys [17] were used. Gettering of oxygen using Zr foil is a well-known technique [18] for reducing the oxy-

author's e-mail: watanabe@riam.kyushu-u.ac.jp

*) This article is based on the presentation at the 25th International Toki Conference (ITC25).

gen concentration in vanadium alloys. This technique is useful for avoiding oxygen pick-up during irradiation. Zr foil (0.002 mm thick) was welded with a rolled V–4Cr–4Ti sheet (approximately 0.15 mm thick) by annealing at 1,373 K for 0.5 h. The V–4Cr–4Ti alloys with and without Zr foil were irradiated at 473 K for 591 h.

3. Results

3.1 Oxygen pick-up during ion irradiation

The microstructural evolution of the laser-welded samples, irradiated at 873 K, at different distances from the bead center is shown in Fig. 1.

At 873 K, fine titanium oxides were observed, even at a dose of 0.75 dpa. These precipitates were identified as Ti(C,O,N) with {100} habit planes [7]. The dose dependencies of the measured number densities and sizes of Ti(C,O,N) in several specimens sliced from different positions are shown in Fig. 2. The number densities of Ti(C,O,N) precipitates formed in the weld metal were approximately one order higher than those formed in the base metal. This density decreased with increasing dose (region 1 in Fig. 2). Well-formed Ti(C,O,N) precipitates were observed at higher-dose levels above 7 dpa (region 2 in Fig. 2). In contrast, almost the same size and density of Ti(C,O,N) precipitates were observed at 12 dpa. The estimated oxygen levels from the measured density and size of the Ti(C,O,N) precipitates are also shown in Fig. 1. For this estimation, TiO was chosen from the Ti(C,O,N) precipitates (NaCl-type crystal structure). The estimated oxygen levels from the microstructure increased with increasing dose and were approximately 20 times higher than those before irradiation at 12 dpa. A similar oxygen pick-up from the vacuum environment using different levels of nitrogen and oxygen samples has been reported in ref [6]. Therefore, for higher-dose levels, the effects of oxygen from the irradiation environment are required to be known, requiring further studies to be done to avoid oxygen pick-up during ion irradiation.

A cross-sectional view of an ion-irradiated sample at 873 K and 7.5 dpa is shown in Fig. 3.

In this figure, the damage-depth profile calculated by TRIM is also shown for comparison. As described in the previous section, Ti(C,O,N) precipitates were detected in the damage region (as shown by 1 in Fig. 3). In contrast, as shown by 2 in this figure, high densities of back-dot im-

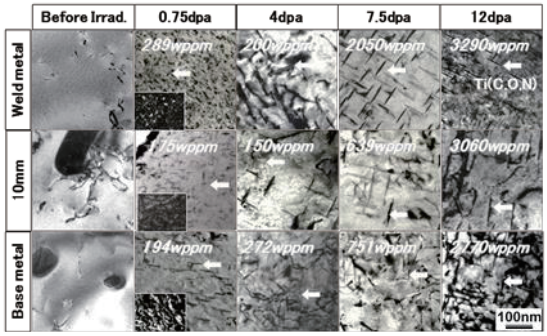

Fig. 1 Microstructural evolution of laser-welded V–4Cr–4Ti alloy irradiated at 873 K at 12 dpa. In the figure, the microstructure of the base metal is also shown for comparison.

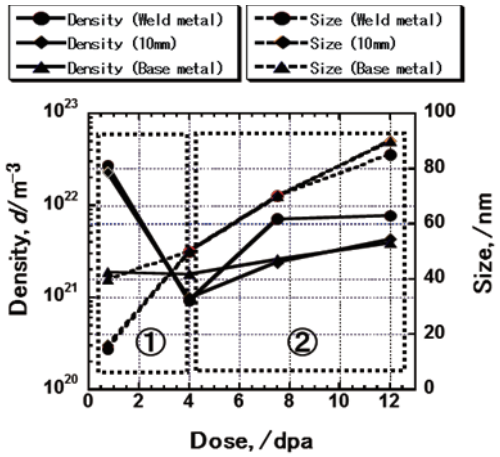

Fig. 2 Dose dependence of the measured densities and sizes of Ti(C,O,N) precipitates at 873 K.

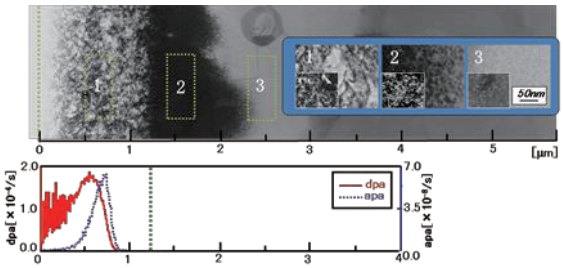

Fig. 3 Cross-sectional view of ion irradiated sample at 873 K at 7.5 dpa. In this figure, the damage-depth profile calculated by TRIM is also shown for comparison.

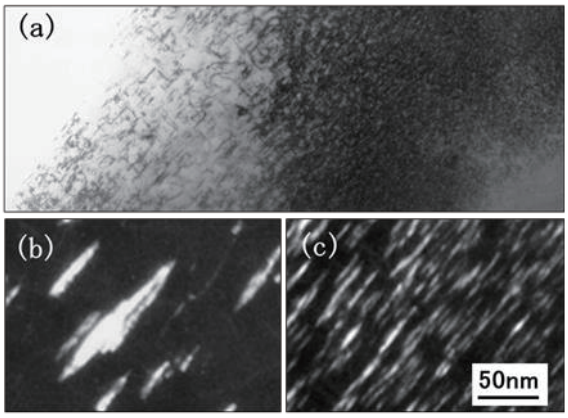

Fig. 4 The microstructure of the sample annealed at 973 K for 30 min. (a) bright-field image at low magnification. (b) and (c) show the higher magnification images of regions 2 and 3, respectively.

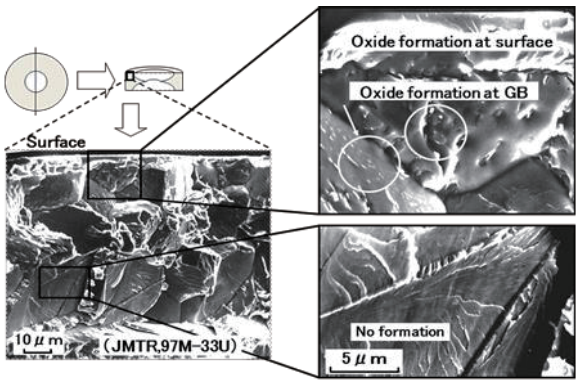

Fig. 5 Fracture surface of broken TEM sample. Neutron irradiation was performed at 573 K for 167 h in JMTR (95M-5U).

ages were observed. To identify these back dots formed in region 2, the sample was annealed in a vacuum environment at 973 K for 30 min. Figure 4 (a) shows a bright field image at a low magnification and Figs. 4 (b) and (c) show higher-magnification images of regions 2 and 3 in Fig. 3, respectively. As shown by these figures, Ti(C,O,N) precipitates in the {100} habit plane were also detected in region 2.

3.2 Oxygen pick-up during neutron irradiation

Oxygen pick-up from the irradiation environment was also observed in previous neutron-irradiation studies performed in JMTR. Irradiated samples suffered serious damage by surface oxidation. For JMTR irradiation, aluminum-specimen capsules were evacuated and high-purity He gas was introduced before sealing these capsules. However, it was very difficult to avoid oxygen pick-up from the He gas in the V–4Cr–4Ti alloy during irradiation. Furthermore, in the beginning of temperature-controlled experiments using JMTR, He gas leakage from the aluminum-specimen capsules occurred and the surfaces of the V–4Cr–4Ti samples were oxidized. The fractured surface of the V–4Cr–4Ti TEM sample, which was irradiated in JMTR (97M-33U) at 573 K for 167 h, is shown in Fig. 5.

For significantly low irradiation-dose, surface oxidation and large oxide precipitates were formed at the grain boundaries. Titanium-oxide formation at the grain boundaries is the main reason for the occurrence of a brittle fracture of the TEM sample. However, these large oxide precipitates were not detected in the middle part of the sample. Figure 6 shows the microstructural evolution of V–4Cr–4Ti alloy irradiated at 573 K. At the beginning of irradiation, small I-type loops and Ti(C,O,N) precipitates were formed. However, with the increase in dose, the number density of Ti(C,O,N) precipitates deceased and well-formed precipitates were observed. The oxygen level estimated from the density and size of the Ti(C,O,N) precipitates was approximately 400 wt ppm, a value that is almost comparable to

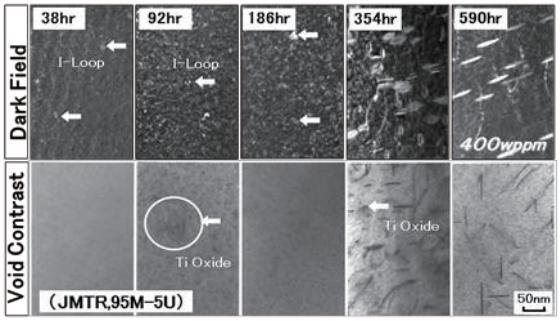

Fig. 6 Microstructural evolution of neutron irradiated V–4Cr–4Ti alloy at 573 K. Upper and lower photos show dark field images and void contrast images, respectively.

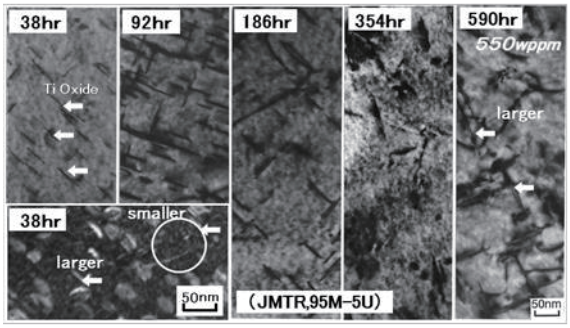

Fig. 7 Microstructural evolution of neutron-irradiated V–4Cr–4Ti alloy at 673 K. A dark field image of the beginning of neutron irradiation (irradiation time: 38 h) is also inserted in the figure.

that estimated before irradiation. Furthermore, the formation of titanium oxide became prominent at higher temperature. As shown in Fig. 7, larger Ti(C,O,N) precipitates (approximately 35 nm) and smaller precipitates (approximately 2 nm) were simultaneously observed at 673 K. With increasing neutron dose, the smaller Ti(C,O,N) precipitates disappeared and well-formed titanium oxides were observed instead. The estimated oxygen level after the end of irradiation was approximately 550 wt ppm. One of the reasons for the strong surface oxidation of V alloys was the leakage of He gas from the aluminum-specimen capsules. To avoid such leakage, improved temperature-control systems and vacuum-sealing methods were employed. Moreover, Zr foils were inserted into the specimen capsules and Zr foil-jointed V–4Cr–4Ti alloys were used for irradiation.

4. Discussions

4.1 Oxygen pick-up from a vacuum environment

Figure 8 shows the microstructure of V–4Cr–4Ti alloys with different specimen thicknesses after annealing at 973 K for 2 h. The upper and lower photos represent the cases of 0.1 mm and 0.27 mm thicknesses, respectively. The measured precipitate densities and sizes of each spec-

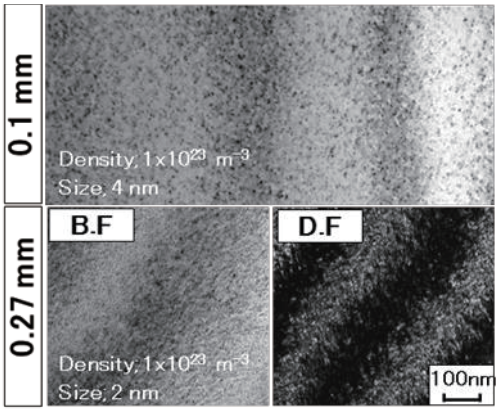

Fig. 8 Microstructure of the V–4C–4Ti alloys with different specimen thicknesses after annealing at 973 K for 2 hr.

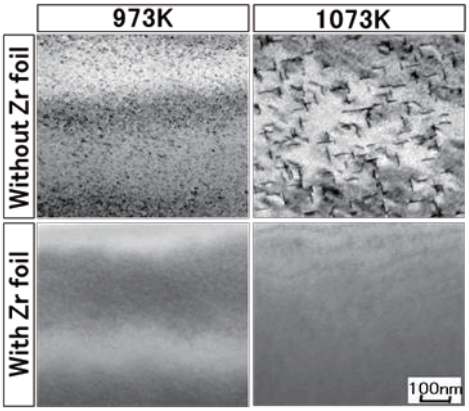

Fig. 9 Microstructure of V–4Cr–4Ti alloy after annealing at 973 K and 1,073 K for 2 hr. The upper and lower photos show the microstructure of the sample without Zr foil (a) and with Zr foil (b), respectively.

imen are shown in the figure. Almost similar densities of the Ti(C,O,N) precipitates were observed in both samples, but much smaller precipitates were detected in the thicker sample. Figure 9 shows the microstructure of the specimen welded with and without Zr foil after annealing at 973 K and 1,073 K for 2 h. By Zr joining, the formation of Ti(C,O,N) precipitates during annealing was completely suppressed. Oxygen diffusivities (D) in V–5Ti alloy are expressed as that in [18, 19].

$$D = 3.1 \times 10^{-4} \exp(-171.8/RT)\ [\mathrm{m}^2/\mathrm{s}], \quad (1)$$

where R and T are the gas constant and annealing temperature, respectively.

The diffusion distance (X) during annealing time (t) is approximately given by

$$X = 2(Dt)^{1/2}. \quad (2)$$

By using equations (1) and (2), the oxygen-diffusion distances at 973 K and 1,073 K for 2 h were measured as 0.07 mm and 0.2 mm, respectively. Therefore, at 973 K,

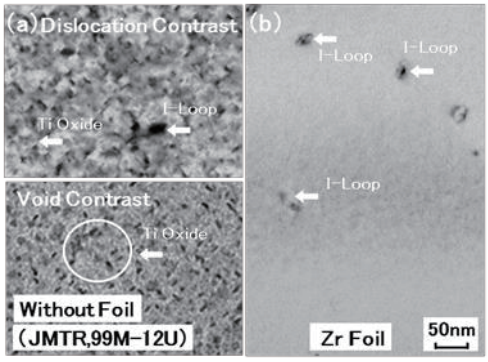

Fig. 10 Microstructure of neutron-irradiated V–4Cr–4Ti alloy at 673 K. (a) Without Zr foil (b) With Zr foil.

TEM samples with 0.1 mm thickness can be affected by oxygen pick-up from the vacuum environment, but not for samples with 0.27 mm thickness. As shown in Fig. 8, almost similar densities of Ti(C,O,N) precipitates were observed in the samples with thicknesses of 0.1 mm and 0.27 mm, but much smaller precipitates were detected in the thicker sample. This means that the oxygen picked up from the vacuum environment enhanced the growth of Ti(C,O,N) precipitates formed at 973 K. In particular, the use of Zr foil promoted oxygen gettering and also acted as a diffusion barrier for oxygen pick-up from vacuum environment. Figure 10 (b) shows the microstructures of Zr-foil-welded V–4Cr–4Ti alloy samples irradiated at 673 K for 591 h (after 1 cycle of irradiation, ~0.1 dpa). The microstructure of the alloy without Zr foil (Fig. 10 (a)) is also shown for comparison. By Zr-welding, the formation of small Ti(C,O,N) precipitates was completely suppressed. Therefore, for higher-irradiation cases, it is concluded that a diffusion barrier such as Zr foil is effective for avoiding additional microstructural changes because of oxygen pick-up.

4.2 Effects of Y on Ti(C,O,N) formation

Y addition to V–4Cr–4Ti alloys is expected to reduce the formation of Ti(C,O,N) precipitates because oxygen is scavenged by Y. The previous copper-ion irradiation on laser-welded V–4Cr–4Ti–0.15Y alloy [20] showed the formation of fine titanium oxides with {100} habit planes at a dose of 0.75 dpa at 873 K. However, for all irradiation doses, the growth of titanium oxides was observed to be suppressed by Y addition. The study also showed that, for welded Y-doped V–4Cr–4Ti alloys, understanding the effects of post-welding heat treatment (PWHT) on the materials is important to reduce their radiation hardening. Furthermore, the addition of Y is very effective for reducing the growth of Ti(C,O,N) precipitates during neutron irradiation at 673 - 873 K and doses up to approximately 0.4 dpa [21]. These results indicate that the scavenging effect by Y addition is effective under relatively low-dose neutron irradiation.

5. Conclusions

Several types of V–4Cr–4Ti alloys were examined to understand the effects of oxygen pick-up in vacuum and He environments during ion- and neutron-irradiation on low-activation vanadium alloys. At 873 K, the densities and sizes of the titanium oxides were drastically changed by oxygen pick-up during irradiation. Zr foil-welding to form a diffusion barrier and Y addition are effective for avoiding additional microstructural changes because of oxygen pick-up.

Acknowledgements

This work was performed with the support and under the auspices of the NIFS Collaboration Research program. This work was also supported in part by the Collaborative Research Program of Research Institute for Applied Mechanics, Kyushu University.

[1] D.L. Simith, B.A. Loomis and D.R. Diercks, J. Nucl. Mater. **135**, 125 (1985).
[2] S.J. Zinkle, H. Matsui, D.L. Simith, A.F. Rowcliffe, E. van Osch, K. Abe and V.A. Kazakov, J. Nucl. Mater. **258-263**, 205 (1998).
[3] T. Nagasaka, H. Takahashi, T. Muroga, T. Tanabe and H. Matsui, J. Nucl. Mater. **283-287**, 816 (2000).
[4] H. Watanabe, T. Arinaga, K. Ochiai, T. Muroga and N. Yoshida, J. Nucl. Mater. **283-287**, 286 (2000).
[5] H. Watanabe, M. Suda, T. Muroga and N. Yoshida, J. Nucl. Mater. **307-311**, 408 (2002).
[6] H. Hatakeyama, H. Watanabe, T. Muroga and N. Yoshida, J. Nucl. Mater. **329-333**, 420 (2004).
[7] H. Watanabe, M. Nagamine, K. Yamasaki, N. Yoshida. Nam-Jin Heo, T. Nagasaka and T. Muroga, Mater. Sci. Forum **475-479**, 1491 (2005).
[8] K. Fukumoto, M. Narui, H. Matsui, T. Nagasaka, T. Muroga, M. Li, D.T. Hoelzer and S.J. Zinkle, J. Nucl. Mater. **386-388**, 575 (2009).
[9] K. Fukumoto, H. Matsui, M. Narui and M. Yamazaki, J. Nucl. Mater. **437**, 341 (2013).
[10] T. Miyazawa, T. Nagasaka, R. Kasada, Y. Hishinuma, T. Muroga, H. Watanabe, T. Yamamoto, S. Nogami and M. Hatakeyama, J. Nucl. Mater. **455**, 440 (2014).
[11] H. Watanabe, N. Yoshida, T. Nagasaka and T. Muroga, J. Nucl. Mater. **417**, 319 (2011).
[12] H. Hatakeyama, T. Muroga, S. Tamura and I. Yamagata, J. Nucl. Mater. **417**, 303 (2011).
[13] H. Hatakeyama, T. Nagasaka, T. Muroga, T. Toyama and I. Yamagata, J. Nucl. Mater. **442**, S346 (2013).
[14] T. Muroga, T. Nagasaka, K. Abe, V.M. Chernov, H. Matsui D.L. Smith, Z.-Y. Xu and S.J. Zinklel, J. Nucl. Mater. **307-311**, 547 (2002).
[15] T. Muroga, T. Nagasaka, A. Iiyoshi, A. Kawabata, S. Sakurai and M. Sakata, J. Nucl. Mater. **283-287**, 711 (2000).
[16] T. Nagasaka, T. Muroga, M.L. Grossbeck and T. Yamamoto, J. Nucl. Mater. **307-311**, 1595 (2002).
[17] K. Fukumoto, T. Morimura, T. Tanaka, A. Kimura, K. Abe, H. Takahashi and H. Matsui, J. Nucl. Mater. **239**, 170 (1996).
[18] K. Abe, A. Kohyama, C. Namba, F.W. Biffen and R.H. Jones, J. Nucl. Mater. **258-263**, 2075 (1998).
[19] H. Nakajima, S. Nagata, H. Matsui and S. Yamaguchi, Philosophical Magazine A **67**, No.3, 557 (1993).
[20] H. Watanabe, A. Higashijima, N. Yoshida, T. Nagasaka and T. Muroga, J. Nucl. Mater. **386-388**, 598 (2009).
[21] H. Watanabe, K. Yamasaki, A. Higashijima, H. Taguma, T. Nagasaka and T. Muroga, to be published in Nuclear Material and Energy.